Chemistry & Biology
Article

Probing the Pore Drug Binding Site of Microtubules with Fluorescent Taxanes: Evidence of Two Binding Poses

Isabel Barasoain,[1] Ana M. García-Carril,[1] Ruth Matesanz,[1] Giorgio Maccari,[2] Chiara Trigili,[1] Mattia Mori,[2] Jing-Zhe Shi,[3] Wei-Shuo Fang,[3] José M. Andreu,[1] Maurizio Botta,[2] and J. Fernando Díaz[1,*]
[1]Centro de Investigaciones Biológicas, Consejo Superior de Investigaciones Científicas, Ramiro de Maeztu 9, 28040 Madrid, Spain
[2]Department of Pharmaceutical and Chemical Technology, Faculty of Pharmacy, University of Siena, I-53100 Siena, Italy
[3]Institute of Materia Medica, Chinese Academy of Medical Sciences, 1 Xian Nong Tan Street, Beijing 100050, China
*Correspondence: fer@cib.csic.es
DOI 10.1016/j.chembiol.2010.02.006

SUMMARY

The pore site in microtubules has been studied with the use of Hexaflutax, a fluorescent probe derived from paclitaxel. The compound is active in cells with similar effects to paclitaxel, indicating that the pore may be a target to microtubule stabilizing agents. While other taxanes bind microtubules in a monophasic way, thus indicating a single type of sites, Hexaflutax association is biphasic. Analysis of the phases indicates that two different binding sites are detected, reflecting two different modes of binding, which could arise from different arrangements of the taxane or fluorescein moieties in the pore. Association of the 4-4-20 antifluorescein monoclonal antibody-Hexaflutax complex to microtubules remains biphasic, thus indicating that the two phases observed arise from two different poses of the taxane moiety.

INTRODUCTION

The clinical success of paclitaxel and docetaxel has triggered the search for compounds with a similar mechanism of action but without their inconveniences (low solubility and development of resistances). This has resulted in the discovery of many compounds with very different chemical structures, epothilones, discodermolides, dyctiostatins, eleutherobin, sarcodyctins, cyclostreptin, laulimalide, and peloruside. These compounds bind to at least three different binding sites. Laulimalide and peloruside reversibly compete among them for a binding site whose location is yet unknown (Pryor et al., 2002; Gaitanos et al., 2004) but not with taxanes, epothilones, discodermolides, dyctiostatins, and eleutherobin, which reversibly compete among them for binding to microtubules (Buey et al., 2005). It has been proven that taxanes and epothilones bind to a site in the luminal face of microtubules (Nogales et al., 1998; Nettles et al., 2004), whereas cyclostreptin, which irreversibly competes with taxane and "taxane binding site" drugs, shares its binding between two locations, the same luminal binding site described for taxanes and epothilones and a site in the external surface of microtubules located in the type I pore (Diaz et al., 2003; Buey et al., 2007), making binding to both sites mutually exclusive.

Taxanes can not directly bind to the internal luminal site; however, they bind very fast to preformed microtubules (Diaz et al., 2003, 2000), thus they have to transiently bind to an easily accessible binding site in their way to the luminal site. Since binding of cyclostreptin to microtubules completely inhibits paclitaxel binding (Buey et al., 2007), the external site of cyclostreptin can be assigned as the initial external binding site for taxanes.

It is not yet known to which one of the sites discodermolides, dyctiostatins, eleutherobin, and sarcodyctins bind: only to the luminal, only to the external, or to both. However, it is easy to observe NMR TR-Noesy of discodermolide and dyctiostatin bound to microtubules (Canales et al., 2008), which indicates a fast kinetic rate of the release step, pointing toward necessary binding to a site different from the slow dissociating luminal site, which could be the pore site. It is possible as well to observe TR-Noesy of docetaxel bound to microtubules (Matesanz et al., 2008), which suggests that taxane dissociation proceeds similarly.

Although it is relatively straightforward to measure and model the interactions of the taxanes and taxane-site binding compounds with the inner luminal binding site (Matesanz et al., 2008; Snyder et al., 2001), almost nothing is known about the nature of the external binding site, just its location in the type I pore and one of the amino acids (Thr220) that is labeled by cyclostreptin on its way to the inner site (Buey et al., 2007). The reason for this is that the equilibrium methods normally used to characterize MSA-microtubule interactions (Buey et al., 2005; Li et al., 2000) cannot provide information about the transient binding to the external site or easily distinguish between binding to the external or the luminal site.

The possible conformations of the external binding site have been recently studied using molecular modeling techniques. The models propose different interactions: in the model of Freedman et al. (2009) the binding site involves both protofilaments of the pore, with the taxane core bound to both β subunits and the side chain bound to the α subunit involved. In the models of Magnani et al. (2009) only one protofilament is involved in the interaction, with the taxane core bound to the β subunit and the side chain bound the α subunit.

A feasible way to study the interactions of ligands with transient sites like the microtubule pore is the kinetic approach

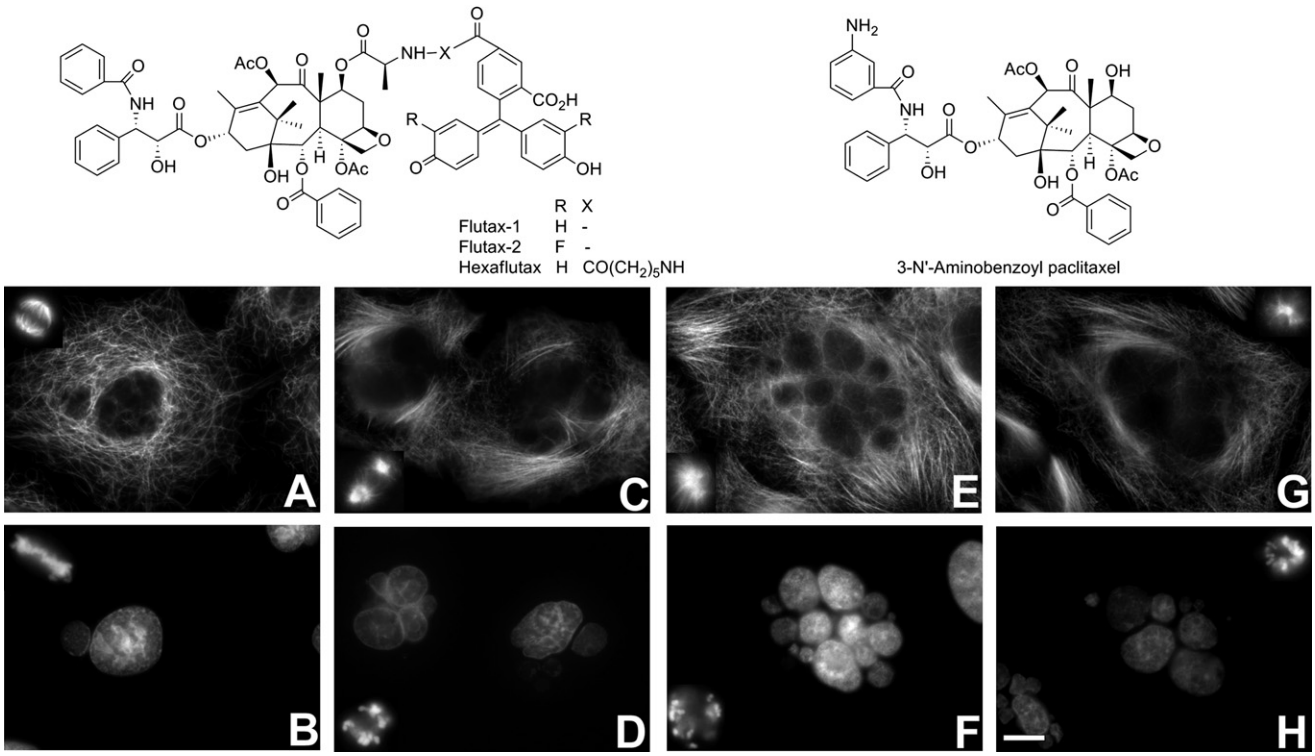

Figure 1. Chemical Structures of the Compounds Used and Effect on Cellular Microtubules

(A–H) Effect of Hexaflutax as compared to Flutax1 and paclitaxel on microtubule network (A, C, E, and G) and nucleus morphology (B, D, F, and H). A549 cells were incubated for 24 hr with DMSO (A and B), 200 nM paclitaxel, 1 μM Flutax-1 (E and F), or 5 μM Hexaflutax (G and H). Microtubules were immunostained with α-tubulin monoclonal antibodies and DNA was stained with Hoechst 33342. Insets are mitotic spindles from the same preparation. The scale bar represents 10 μm. All panels and insets have the same magnification.

(Diaz et al., 2003, 2000). The kinetics of binding and dissociation of ligands to microtubules should provide information about the interaction of the compound with the pore site. In this work the interaction of taxanes with microtubules has been characterized using two probes labeled at different parts of the molecule (Figure 1), C7 in the north face and the C13 side chain, which has a large contribution to the energy of binding (Matesanz et al., 2008). The first probe is Hexaflutax (Diaz et al., 2005), a fluorescent taxane derivative tailored to have a separation between the fluorescein and the taxane moieties allowing binding of a monoclonal antibody [4-4-20 (Kranz and Voss, 1981)] directed against the fluorescein moiety, as long as the taxane moiety is bound to an external site, but not if the taxane is bound to the internal site. It has been proven that this compound either bound or not to the antibody remains at the external site when bound to microtubules (Diaz et al., 2005). The other compound studied was 3′-N-m-aminobenzamido-3′-N-debenzamidopaclitaxel (N-AB-PT) (Li et al., 2000), a taxane derivative that carries a fluorescent aminobenzamido group at the C13 side chain. The results indicate that both fluorescent taxanes bind to the pore site with an affinity of the order of micromolar. While N-AB-PT binds in a single type of site similar to C7 fluorescent-labeled paclitaxel analogs, i.e., Flutax-1 and Flutax-2, the presence of the long aliphatic chain in Hexaflutax allows a second possibility of binding of the compounds to this site, which results in the observation of a biphasic binding kinetics.

RESULTS

Paclitaxel-like Cellular Effects of Hexaflutax

In previous work (Diaz et al., 2005) we had found that Hexaflutax binds to the external site of microtubules. Thus we wanted to characterize its cellular effects in tumor cells to detect any possible differential effect between binding to the pore and the luminal sites. First, cytotoxicity in A2780 and A2780AD as compared to paclitaxel and the two other fluorescent taxanes, Flutax-1 and Flutax-2, was determined. Hexaflutax is less active with IC_{50} in A2780 cells of 2.3 μM as compared with the other fluorescein-labeled compounds, Flutax-1 and -2 (IC_{50} 0.26 μM and 0.8 μM, respectively), all fluorescent taxanes being significantly less active than paclitaxel (IC_{50} 1.1 nM). The three fluorescent taxanes are inactive against P-glycoprotein-overexpressing A2780AD cells at the highest concentration (20 μM) tested (IC_{50} paclitaxel 1.1 μM).

We also studied the effect of Hexaflutax on cellular microtubules. Treatment of A549 cells for 24 hr with either paclitaxel (200 nM), Flutax-1 (1 μM), or Hexaflutax (5 μM) gave rise to the characteristic cytoplasmic microtubule bundles as well as to aberrant mitosis (monopolar spindles) and to micronucleated cells (Figure 1), as expected from the microtubule-stabilizing agent activity observed for the ligand. Hexaflutax is able to in vitro induce tubulin assembly in conditions in which tubulin itself is unable to assemble, i.e., in 10 mM phosphate

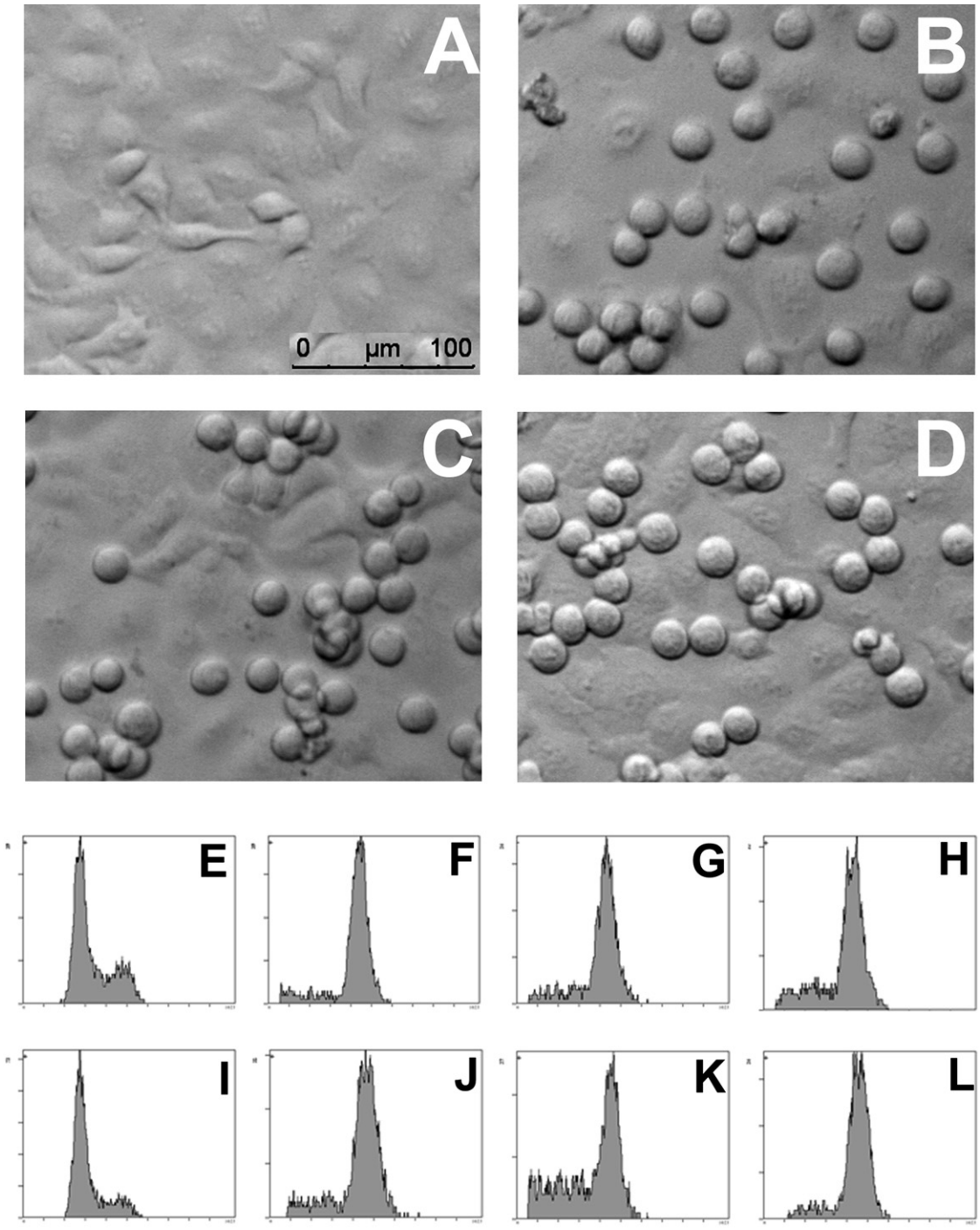

Figure 2. Effect of Taxanes in Morphology and Cell Cycle of A549 Cells

(A–D) Morphology of A549 cells after treatment with paclitaxel, Flutax-1, and Hexaflutax. A549 cells were incubated for 20 hr with either DMSO (A), 20 nM Taxol (B), 2 μM Flutax-1 (C), and 4 μM Hexaflutax (D).

(E–L) Effect on A549 and A2780 cell cycle of Hexaflutax as compared with Taxol and Flutax-1. A549 cells were incubated for 20 hr with DMSO (E), 20 nM Taxol (F), 2 μM Flutax-1 (G), and 4 μM Hexaflutax (H) and A2780 cells with DMSO (I), 30 nM Taxol (J), 2 μM Flutax-1 (K), and 10 μM Hexaflutax (L).

buffer, 1 mM EDTA, 6 mM $MgCl_2$, and 0.1 mM GTP (pH 7.0) (Evangelio, 1999).

We next studied whether Hexaflutax was able to accumulate cells in the G2+M phase of the cell cycle as paclitaxel and the other two fluorescent derivatives do. A549 lung carcinoma cells as well as A2780 ovarian carcinoma cells were incubated for 20 hr in the presence of these three drugs and their cell morphology was examined by DIC microscopy (Figures 2A–2D)

before processing cells for the cell cycle experiment. Most A549-treated cells and A2780 cells (data not shown) were rounded mitotic cells as compared to the control cells that were spread epithelial-like adherent cells with few mitotic cells. 20 nM Taxol, 2 μM Flutax-1, and 4 μM Hexaflutax and 30 nM Taxol, 2 μM Flutax-1, and 10 μM Hexaflutax accumulate cells in the G2+M phase of the cell cycle in both A549 and A2780 cells, respectively (Figures 2E–2L), demonstrating that the binding of taxanes to the pore and to the lumenal sites produce the same biological effect in cells.

Equilibrium of Binding of Fluorescent Taxoids to Stabilized Microtubules

The binding constant of Hexaflutax to the taxoid site in crosslinked microtubules was measured by the increase of fluorescence anisotropy upon binding (r_{free} 0.06 and r_{bound} 0.18) (Figure 3A and Table 1) and by centrifugation (data not shown). The results indicate 1:1 stoichiometry and a micromolar order affinity $K_{25°C}$ of 1.13 ± 0.01 × 10^6 M^{-1} (anisotropy measurements) and $K_{25°C}$ of 2.1 ± 0.3 × 10^6 M^{-1} (centrifugation measurement).

The binding is exothermic with both favorable enthalpic (ΔH_{app} = −25 ± 2 kJ mol^{-1}) and entropic (ΔS_{app} = +31 ± 7 J mol^{-1} K^{-1}) contributions to the free energy of binding ($\Delta G_{app\ 35°C}$ = −34.8 ± 0.5 kJ mol^{-1}) (from data in Table 1).

Binding of N-AB-PT to crosslinked microtubules indicates a single site with an equilibrium binding constant of $K_{25°C}$, 5.0 ± 0.6 × 10^6 M^{-1}, independently of the method used (data not shown).

Kinetics of Binding and Dissociation of Fluorescence to the Taxoid Site

Binding of Hexaflutax to the taxoid site is accompanied by a 40% decrease in the intensity of the fluorescence of the probe (Diaz et al., 2005), thus the kinetics of binding (Figures 3B–3D) and dissociation (Figure 3E; see Figure S1 available online) was studied using stop-flow techniques.

Opposite to what has been previously observed for the closely related fluorescent taxoids Flutax-1 and Flutax-2, the kinetics of association of Hexaflutax to the taxoid site were inhomogeneous (Figure 3B) [χ2 (1 phase) = 113.17; χ2 (2 phases) = 17.01; χ2 (3 phases) = 17.00]. The kinetics of association shows a majoritarily fast and a minoritarily slow phase (Figure 3C) whose amplitude decreases with the concentration of sites to become negligible at the higher concentrations of sites studied (Figure 3D). The values of the observed kinetic rate constants are linearly dependent on the observable range (note that the slow phase disappears at high binding site concentration) of the total concentration of sites, which indicates pseudofirst order bimolecular reactions (Table 1 and Figure 3C).

The observation of two different kinetic constants (two kinetic phases) for the process can be due to two different reasons. Either we are observing two simultaneous reactions with different kinetic rates or two subsequent reactions. In the first case, the two simultaneous reactions are bimolecular reactions, which is reflected in the fact that both kinetic rates observed are linearly dependent on the site concentration. In the second, one of the reactions is a monomolecular reaction and one of the kinetic rates observed will follow a non-linear dependence on the site concentration (Gutfreund, 1995). The fact that two bimolecular reactions are observed in this case indicates that two simultaneous binding reactions of Hexaflutax to microtubules are observed.

The kinetics of dissociation of Hexaflutax from the site are also inhomogeneous, showing two kinetic rates similar in amplitude (Figure 3E and Table 1; Figure S1).

The fact that the slow phase of the association kinetics disappears at high site concentrations indicates that the inhomogenity arises from two different classes of binding sites, some easily accessible and others more difficult to access. The proportion between amplitudes of the slow and the fast phases of the dissociation kinetics indicates that the proportion of both sites is equal.

The thermodynamic analysis of the interaction shows that both putative binding sites would have very similar thermodynamic behavior (Table 1) with similar activation energies kinetic for the association and dissociation, the kinetically determined binding enthalpy (ΔH_{fast} = −33 ± 9 kJ mol^{-1}; ΔH_{slow} = −38 ± 9 kJ mol^{-1}) being close to the value determined from equilibrium measurements (ΔH_{app} = −25 ± 2 kJ mol^{-1}).

Although it is difficult to determine the affinities of both binding sites by equilibrium binding assays, the value can be deduced from kinetic measurements of dissociation in condition of excess of binding sites, since the compound will preferentially bind to the sites with higher affinity. The kinetics of dissociation of 3 μM 7-Hexaflutax from 10 μM binding sites have been measured at 25°C and 35°C (Table 2). The ratio between the amplitudes of the fast and the slow phase increases from 1:1 to 2:1, implying that fast binding site have a higher affinity. The binding affinities can be calculated from the ratio of the phases and the apparent equilibrium binding constant (Table 1) and are in very good agreement with those that can be calculated from the kinetic binding data (Table 1), thus supporting the one step model of binding to two overlapping binding sites and the absence of a second binding step.

The kinetics of association and dissociation of Hexaflutax were followed using fluorescence anisotropy measurements (Figure S2) to detect a second step of the reaction without change of fluorescence intensity as is observed for Flutax-1 and Flutax-2 (Diaz et al., 2000). Although the noise of the signal does not allow distinguishing between monophasic and biphasic kinetics, the observed kinetic rate constant is very similar to that simultaneously measured by fluorescence intensity, thus indicating that the same process is observed using both techniques, as would be expected if the compound is not internalized toward the inner site.

The kinetics of binding of another fluorescent taxane derivative, 3-N′-aminobenzoyl paclitaxel (Li et al., 2000), in which the fluorescence probe is the benzoyl side chain modified by the introduction of an amine group, were also used to explore the structure of the paclitaxel external binding site. Since the compound has been reported to have two different kinds of binding sites depending on the nucleotide bound to the exchangeable site (Li et al., 2000), all experiments were done with crosslinked stabilized microtubules that contain GDP in the exchangeable site.

Contrary to binding of 7-Hexaflutax and similarly to Flutax-1 and Flutax-2, N-AB-PT shows a single type of binding site.

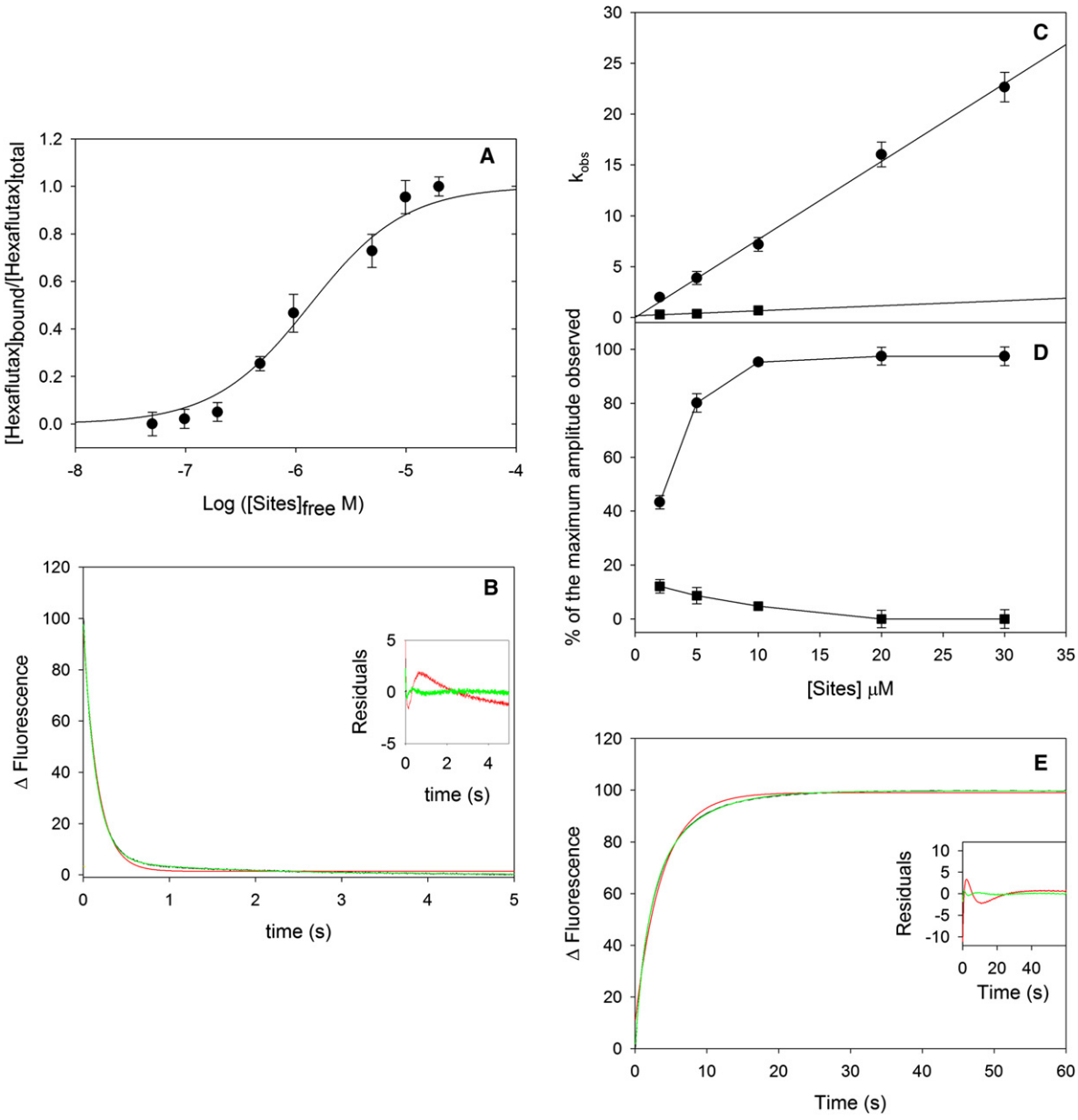

Figure 3. Binding of Hexaflutax to Microtubules

(A) Titration curve of 100 nM Hexaflutax with taxoid sites in stabilized microtubules at 35°C. Solid line, fit of the data to a single binding site model.

(B) Kinetics of association of Hexaflutax to its site in microtubules at 35°C. In the stopped flow device a solution containing 200 nM Hexaflutax was mixed with 10 μM taxoid sites, final concentrations. The curve (black line) is fitted either to a single exponential (red line) or to a double exponential (green line). Inset residuals of the fitting to a single (red line) and a double exponential (green line).

(C) Dependence on the concentration of taxoid sites of the two observed rate constants for Hexaflutax binding at 35°C for the binding reaction.

(D) Dependence on the concentration of taxoid sites of the amplitude at 35°C of the two observed kinetic phases of the binding reaction.

(E) Kinetics of dissociation of Hexaflutax from its site in microtubules at 35°C. In the stopped flow device a solution containing 4 μM Hexaflutax bound to 5 μM taxoid sites was mixed with 100 μM docetaxel, final concentrations. The curve (black line) is fitted either to a single exponential (red line) or to a double exponential (green line). Inset residuals of the fitting to a single (red line) and a double exponential (green line). Error bars are standard errors of the measurement.

Although the observed kinetics are biphasic as was observed for Flutax-1 binding to MAP-containing microtubules (Diaz et al., 2003), the second kinetic phase has a non-linear concentration dependence with the site concentration (Figures 4A and 4B). A biphasic kinetics with a kinetic rate linearly dependent on the site concentration and a second kinetic rate with a non-linear dependence as described, can be explained by a scheme of coupled reactions with comparable rate constants (Strehlow and Knoche, 1977; Diaz et al., 1997). The first reaction can be assigned to the bimolecular binding of the ligand to the site, which has a kinetic rate constant at 35°C of 3.9 ± 0.7 × 10^5 M^{-1} s^{-1} while the second one should be the monomolecular

Table 1. Equilibrium, Kinetic, and Thermodynamic Parameters of Binding of Hexaflutax to Its Site in Microtubules

Equilibrium Constants	25°C	27°C	30°C	32°C	35°C	37°C	40°C	42°C
K ($\times 10^5$ M^{-1})[a]	11.3 ± 0.1	9.6 ± 1.2	9.2 ± 1.2	8.4 ± 1.3	7.2 ± 1.1	7.2 ± 1.3	6.4 ± 1.3	6.6 ± 1.3
K ($\times 10^5$ M^{-1})[b]	20.6 ± 2.2	ND	19.5 ± 2.5	ND	11.9 ± 0.6	14.0 ± 1.7	ND	11.0 ± 0.9
K ($\times 10^5$ M^{-1})[c]	6.5 ± 3.2	ND	6.1 ± 4.0	ND	3.4 ± 2.0	3.8 ± 1.7	ND	3.1 ± 1.4
Kinetic Constants	25°C		30°C		35°C	37°C		42°C
Association fast k^+ ($\times 10^5$ M^{-1} s^{-1})	4.12 ± 0.28		6.35 ± 0.75		7.35 ± 0.30	10.37 ± 1.10		13.90 ± 1.00
Association slow k^+ ($\times 10^5$ M^{-1} s^{-1})	0.36 ± 0.15		0.51 ± 0.23		0.59 ± 0.29	0.75 ± 0.32		1.01 ± 0.43
Dissociation fast k^{-1} ($\times 10^{-1}$ s^{-1})	2.00 ± 0.07		3.25 ± 0.03		6.20 ± 0.08	7.39 ± 0.08		12.60 ± 0.09
Dissociation fast Amplitude %	49 ± 3		52 ± 1		52 ± 1	56 ± 1		61 ± 1
Dissociation slow k^{-1} ($\times 10^{-1}$ s^{-1})	0.55 ± 0.03		0.83 ± 0.1		1.69 ± 0.08	1.97 ± 0.03		3.25 ± 0.03
Dissociation slow Amplitude	51 ± 3		48 ± 1		48 ± 1	44 ± 1		38 ± 1

$Eak+_{fast}$ = 55 ± 6 kJ mol^{-1}; $Eak+_{slow}$ = 46 ± 4 kJ mol^{-1}; $Eak-_{fast}$ = 86 ± 3 kJ mol^{-1}; $Eak-_{slow}$ = 84 ± 5 kJ mol^{-1}; ΔH_{fast} = −33 ± 9 kJ mol^{-1}; ΔH_{slow} = −38 ± 9 kJ mol^{-1}; ΔH_{app} = −25 ± 2 kJ mol^{-1} (from equilibrium measurements). Error bars are standard errors of the measurement.
[a] Data from equilibrium measurements.
[b] Data from kinetic measurements, fast phase.
[c] Data from kinetic measurements, slow phase.

rearrangement of the complex formed with a rate constant of 3.0 s^{-1}. This two step reaction is similar to that observed for Flutax-1 and Flutax-2 binding to microtubules (Diaz et al., 2000) and different to the one observed for Hexaflutax in this work.

Kinetics of Association and Dissociation of 4-4-20-Bound Hexaflutax

Hexaflutax, 4-4-20 antibody, and microtubules form a ternary complex with the taxane moiety of Hexaflutax bound to an external exposed site (Diaz et al., 2000) and the fluorescein moiety quenched by the antibody. The kinetics of binding and dissociation of the binary 4-4-20-Hexaflutax complex to its site in the microtubules have been measured at 35°C and compared with Hexaflutax kinetics.

The presence of the 4-4-20 antibody bound to Hexaflutax does not modify the existence of two phases for the binding reaction (Figure 4C) although it slows down both the two observed phases of association and dissociation (k_+fast 35°C Hexaflutax 7.35 ± 0.30 × 10^5 M^{-1} s^{-1}, k_+fast 35°C 4-4-20-Hexaflutax complex 0.67 ± 0.16 × 10^5 M^{-1} s^{-1}, k_+slow 35°C Hexaflutax 0.59 ± 0.30 × 10^5 M^{-1} s^{-1}, k_+slow 35°C 4-4-20-Hexaflutax complex 0.16 ± 0.02 × 10^5 M^{-1} s^{-1}). It can be observed that the ratio between the two kinetic phases decreases more slowly than in the case of Hexaflutax, which indicates that the difference in accessibility of the two binding sites should be smaller.

Table 2. Kinetics Constants of Dissociation of Hexaflutax Complex from Crosslinked Microtubules in Conditions of Excess of Binding Sites

	25°C	35°C
Fast phase k^{-1} ($\times 10^{-1}$ s^{-1})	2.6 ± 0.3	5.1 ± 0.2
Fast phase amplitude	65 ± 3	67 ± 2
Slow phase k^{-1} ($\times 10^{-1}$ s^{-1})	0.60 ± 0.05	1.1 ± 0.1
Slow phase amplitude	35 ± 4	32 ± 2
Kb_{fast}[a] (M^{-1})	25 ± 3 × 10^5	11 ± 2 × 10^5
Kb_{slow}[a] (M^{-1})	7.1 ± 1.2 × 10^5	4.3 ± 0.8 × 10^5

[a] Calculated from the ratio of phases.

The dissociation kinetics of the 4-4-20-Hexaflutax-microtubule complex are biphasic with approximately equal fast and slow phases (51 ± 1% fast phase and 49 ± 1% slow phase) as was the case for the Hexaflutax microtubule complex. The velocity of the observed phases is approximately three times slower than that of the Hexaflutax-microtubule complex (k_{-fast} 35°C Hexaflutax 6.20 ± 0.08 × 10^{-1} s^{-1}, k_{-fast} 35°C 4-4-20-Hexaflutax complex 2.78 ± 0.05 × 10^{-1} s^{-1}, k_{-slow} 35°C Hexaflutax 1.69 ± 0.08 × 10^{-1} s^{-1}, k_{-slow} 35°C 4-4-20-Hexaflutax complex 1.27 ± 0.06 × 10^{-1} s^{-1}).

Molecular Modeling

In a previous work we modeled the possible binding sites for paclitaxel in the type I pore of the microtubule (Magnani et al., 2009). Within this region, constituted by four subunits of tubulin belonging to different heterodimers (Figure S3), two possible ligand binding sites were identified due to the rearrangement of the loop between helixes H6 and H7. Accordingly, two binding modes for taxanes were proposed, in close neighborhood, allowing for exchange between them.

In this work we used molecular modeling procedures to study binding of Hexaflutax within the type I pore. Direct docking of the compound to the site leads to ambiguous results due to the large conformational freedom of the spacer; thus we carried out a fragment-based approach to model the possible binding conformation of Hexaflutax, starting from the docking poses of paclitaxel already described (Magnani et al., 2009).

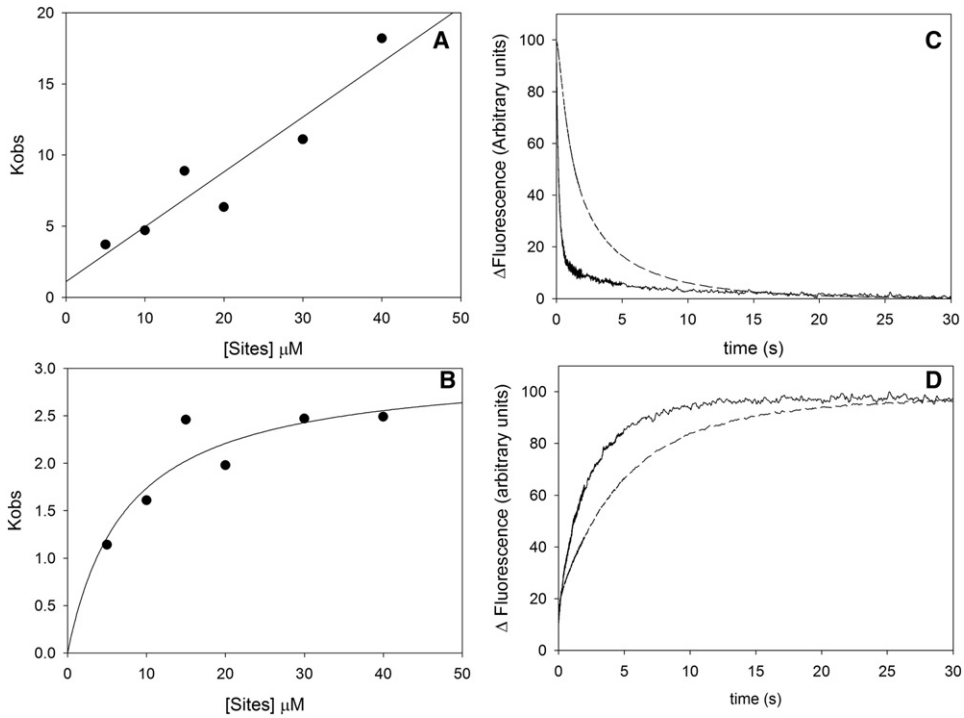

Figure 4. Binding of N-AB-PT and 4-4-20-Hexaflutax Complex to Microtubules

(A and B) Kinetics of dependence on the concentration of taxoid sites of the fast (A) and slow (B) observed rate constants for N-AB-PT binding to crosslinked stabilized microtubules at 35°C.

(C) Comparison between the kinetics of association of Hexaflutax and the 4-4-20-Hexaflutax complex to its site in microtubules at 35°C. In the stopped flow device, a solution containing 500 nM Hexaflutax (solid line; average of two shots) or 500 nM Hexaflutax and 750 nM 4-4-20 antibody (dashed line; average of ten shots) was mixed with 10 μM taxoid sites, final concentrations.

(D) Kinetics of dissociation of Hexaflutax from its site in microtubules at 35°C. In the stopped flow device a solution containing 2 μM Hexaflutax (solid line; average of two shots) or 2 μM Hexaflutax plus 2.5 μM 4-4-20 (dashed line; average of ten shots) bound to 2.5 μM taxoid sites was mixed with 100 μM docetaxel, final concentrations. Note that the curves are scaled to 100 since the fluorescence of the free Hexaflutax is five times larger than that of the 4-4-20 Hexaflutax complex.

The first tested hypothesis was that the inhomogenity observed of the binding was due to possible differences between the most common isotypes of human β-tubulin, namely, βI and βIII. Thus, we modeled paclitaxel on each subtype obtaining a total of four complexes (two possible binding modes and two isotypes). The two binding modes previously found were kept unchanged, which was expected due to the highly conserved sequences of the binding site among isotype βI and βIII.

Then, in order to study the possibility that the inhomogenity observed arises from different binding poses of the fluorescein moiety in the binding site, a preliminary mapping of the whole pore region with only the fluorescent moiety of Hexaflutax molecule was performed by means of the blind docking approach (Hetenyi and van der Spoel, 2002). In a preliminary investigation, carried out toward the free protein, we found two possible binding modes. The most representative binding mode for the fluorescent moiety of Hexaflutax was found in the inner wall of microtubules, between two β subunits. No differences between the βI and βIII isotypes were found in this region. A second alternative binding site for the fluorescent moiety of Hexaflutax was found in the outer wall of microtubules.

The docking of the fluorescein moiety in the binding site was then repeated toward the four paclitaxel/tubulin complexes previously determined, keeping the paclitaxel molecule frozen in the binding conformations already described. The binding modes for the fluorescent moiety were approximately the same as obtained without paclitaxel in the pore site. Two large clusters of conformations were found, collecting a significant proportion of the total conformations docked. The highly populated clusters were generally at the lowest free energy of binding (Figure S4A) and were representative for the interaction of the fluorescent moiety in the inner wall of the type I pore. On the contrary, lower populated clusters described the interaction with the outer side of the pore.

The well defined inner binding cavity used by fluorescein is constituted by residues Lys216, Thr218, and Gly277 of subunit β1 and Arg77, Pro87, Asp88, and Phe90 of subunit β2; a difference in amino acid composition between βI and βIII isotypes can be found in the loop H6-H7, changing Thr218 to Ala218. This difference, however, does not affect the ligand binding conformation. On the contrary, the outer side of the pore lacks a defined interaction groove that results in a large scattering of binding poses for the fluorescent moiety.

Interestingly, the analysis of the docking-based binding pose calculated for the fluorescent moiety toward the paclitaxel/tubulin complexes shows, in all cases, a close proximity between the two moieties allowing a direct linkage that could reproduce the whole Hexaflutax by means of this fragment-based strategy.

In order to do so the linker between paclitaxel and the fluorescent moiety was docked in the ternary complexes (paclitaxel, fluorescein, and tubulin) calculated in the previous step, after defining two anchor positions for covalent bonding on each substructure (Figure S4B). A slight energy minimization process was then performed for all the complexes to relax the linker within the whole Hexaflutax, resulting in the models presented in Figure 5 when the ternary complex used was that with the fluorescein placed in the inner wall of the microtubule and those presented in Figure S5 when the ternary complex used was that with the fluorescein placed in the outer wall of the microtubule. However, it should be pointed out that the contribution of the fluorescein moiety to the free energy of binding should be very low, because the equilibrium binding constant of the 4-4-20 antibody-Hexaflutax to microtubules is three times higher than those of Hexaflutax (Diaz et al., 2005) (although an exact calculation of its contribution cannot be done since the close proximity of tubulin and antibody residues will result in unspecific interactions). Thus, it is very likely that the fluorescein moiety is distributed between the unbound state and the inner and outer bound positions as indicated by the fact that microtubule-bound Hexaflutax fluorescence is rapidly quenched by the antibody.

Free energies of binding of Hexaflutax with the fluorescein moiety placed in the two different possibilities were further calculated with the local search algorithm implemented on AutoDock4. A mean difference of 13.96 KJ/mol between internal and external binding modes was found (Table S1). This difference was probably due to the most favorable Van der Waals interactions exploited by Hexaflutax in the unique inner site, with respect to the scattered conformations observed in the outer region.

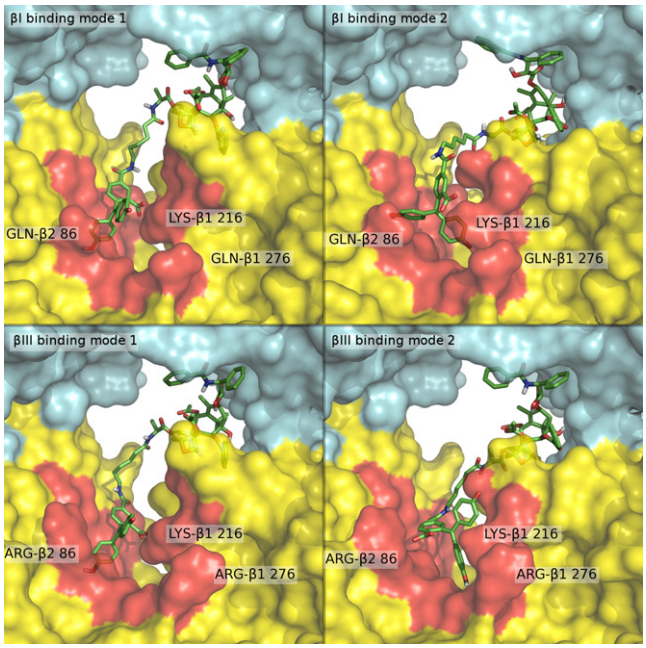

Figure 5. Docking-Based Binding Modes of Hexaflutax in the Binding Site

These conformations were obtained by a fragment-based approach starting from two conformations of the taxane moiety (binding mode 1 and binding mode 2) toward isotypes βI and βIII of tubulin. The two top panels show the βI complexes, whereas the bottom panels show the βIII complexes, all viewed from the inside of the microtubule. α and β subunits are colored in cyan and yellow, respectively; the hexaflutax molecule is shown in green sticks. The residues mostly involved in the interaction with the fluorescent moiety of hexaflutax are highlighted by red surfaces.

DISCUSSION

Hexaflutax is a fluorescent probe of the pore site of microtubules, which is not internalized to the luminal site. The compound is cytotoxic with similar cellular effects to the other taxanes studied, indicating that compounds binding to the external site have the same microtubule stabilizing activity and they kill cells through the blocking of microtubule dynamics. Thus the external binding site can be the target of specifically designed antitumor drugs. This compound has 35 times less affinity than the compound with a shorter spacer between the taxane and the fluorescein group (Flutax-1) (Diaz et al., 2000), suggesting a free energy of around −9 kJ/mol for the internalization of the taxanes.

Hexaflutax Binds Inhomogeneously to the Pore Site of Microtubules

The main difference observed between the binding of Hexaflutax to microtubules and that of other taxanes, Flutax-1 and Flutax-2, is the existence of biphasic behavior in both the association and dissociation of each compound from/to its site. This biphasic behavior arises from the interaction of the compound with the external site and not from any possible simultaneous binding with both the internal and the external sites, since this is also observed when any possible interaction with the internal site is blocked with an antibody.

Kinetic analysis indicates that the inhomogenity arises from two kinds of binding sites, which may be proposed to be: (a) different overlapping binding sites (either from the paclitaxel or the fluorescein moiety), (b) sites formed by different tubulin isoforms, or (c) two different pores of microtubules. However, hypothesis c would be very unlikely since the observed stoichiometry is very close to 1. A fourth, alternative hypothesis would be (d) the existence of two different types of binding sites in microtubules, a high affinity one in GTP tubulin and a low affinity one in GDP-bound tubulin as previously described by Li et al. (2000) for N-AB-PT. This possibility can be discarded because with the stabilized microtubules used, which have GDP bound to the exchangeable nucleotide site, we can only observe a single type of binding site with binding affinity of the order of 10^7 M^{-1} for N-AB-PT.

It can then be assumed that the inhomogenity of Hexaflutax arises from either two binding modes to the same site (with one of the modes not allowed in the case of Flutax-1 and Flutax-2) or from binding to two different tubulin isoforms, with binding parameters similar for Flutax-1 and Flutax-2, but not for Hexaflutax. Since the kinetic constant of the fast phase from association is very similar in the case of all compounds studied (k_{+1} 35°Flutax-1 6.12 ± 0.22 × 10^5 M^{-1} s^{-1}, Flutax-2 5.66 ± 0.50 × 10^5 M^{-1} s^{-1}, N-AB-PT 3.9 ± 0.7 × 10^5 M^{-1} s^{-1}, Hexaflutax 7.35 ± 0.30 × 10^5 M^{-1} s^{-1}) and the taxane moiety of Hexaflutax and Flutax-1 and Flutax-2 are identical, it is straightforward to assign this fast phase of association to the interaction that Flutax-1 and Flutax-2 have in their association.

The remaining possibilities were studied using molecular modeling techniques. Docking studies described two possible binding poses for the paclitaxel moiety of Hexaflutax located on the inner surface on the type I pore of tubulin, at the interface of two β subunits [similar to those previously described by Magnani et al. (2009)] and two possible binding poses for the fluorescein moiety located in the inner and the outer surface of the microtubule wall. The small differences in the sequences of the βI and βIII tubulin in this area resulted in identical dockings irrespective of the tubulin isoforms forming the pore and suggest that this possibility (b) may be discarded.

Since blocking of the fluorescent moiety with a large molecule does not result in changes of the inhomogeneous kinetic behavior, the only remaining hypothesis would be that the two observed bimolecular reactions correspond to the two different binding modes of the paclitaxel moiety. While N-AB-PT, Flutax-1, and Flutax-2 bind in only one possible way, the long aliphatic side chain of Hexaflutax placed at position 7 may stabilize the second, less energetically favored, possible binding pose through interactions with the α subunit of the pore (binding mode II in Figure 5 and Figure S5), making it observable.

SIGNIFICANCE

This work presents for the first time a new pharmacological target in microtubules, the pore site of microtubule stabilizing agents, to which taxanes transiently bind on its way to the luminal site. The use of a fluorescent analog, Hexaflutax, designed to exclusively bind to this pore site has shown that binding of a taxane to this pore site results in cytotoxic effects and cell cycle arrest, identical to those produced by classical taxanes, e.g., paclitaxel and docetaxel, which bind to the luminal site of the microtubule.

The interaction of Hexaflutax with the site has been studied using fast kinetic techniques, allowing the observation of two different possibilities of interaction of drugs with the pore binding site. This pore binding site might be an intermediate site to which a large number of paclitaxel biomimetics with similar microtubule stabilizing agent activity but completely different chemical structures, e.g., paclitaxel, epothilone, discodermolide, and cyclostreptin, bind. While paclitaxel and epothilone are known to be internalized, cyclostreptin labels both the pore and the luminal site and it is not known whether dyctiostatin and discodermolide are internalized. Thus, the pore site could provide additional binding possibilities to microtubule stabilizing agents that may justify the apparent promiscuity of the previously thought single paclitaxel site in microtubules.

EXPERIMENTAL PROCEDURES

Tubulin, Taxoids, and Antibodies

Purified calf brain tubulin and chemicals were as described previously (Andreu, 2007; Diaz and Andreu, 1993). Stabilized mildly crosslinked microtubules were prepared as previously described (Diaz et al., 2000, 2003); their nucleotide content was measured by $HClO_4$ extraction of microtubule pellets and quantified by FPLC using a Vydac 320IC4 ion exchange column developed at 2 ml/min with a 20 min sodium phosphate (pH 2.8 adjusted with acetic acid) gradient from 25 to 125 mM in an Äkta purifier (GE Healthcare) and was found to be 100% GDP.

Paclitaxel was provided by the National Institutes of Health, Docetaxel (Taxotere) was provided by Aventis, and 7-Hexaflutax (Diaz et al., 2005) was provided by F. Amat-Guerri. N-AB-PT (Li et al., 2000) was newly synthesized in milligram scale as described in supplemental information. Its ^{1}H and ^{13}C NMR spectra were recorded on Varian VNS-600 (600 MHz), Varian Mercury-400 (400 MHz), and Varian Mercury-300 (300 MHz) NMR instruments. Mass spectrometry data were recorded on Agilent 1100 LC/MSD (ESI) LC-MS or US LCQ MS instruments. ^{1}H and ^{13}C NMR and mass spectrometry data were found to be coincident with data previously published (Li et al., 2000). Thin layer and flash column chromatography were performed with silica gel GF254 and H (300–400 mesh), respectively, both of which are products from Qing Dao Oceanic Chemical Engineering Factory. All reagents are commercially available and used without further purification. HPLC analysis of the compound was performed in an Agilent 1100 series instrument using a Supercosil, LC18 DB, 250 × 4.6 mm, 5 mm bead diameter column developed in a gradient from 50%–80% (v/v) acetonitrile in water at a flow rate of 1 ml min^{-1}, following absorbance at λ = 220 nm. Its purity was found to be more than 98%.

Taxoids were dissolved in DMSO and their concentrations were measured spectrophotometrically as described previously (Diaz and Andreu, 1993; Diaz et al., 2000, 2003; Evangelio et al., 1998; Li et al., 2000).

4-4-20 antifluorescein monoclonal mouse IgG (Kranz and Voss, 1981) was a gift from E.W. Voss Jr. (University of Illinois at Urbana-Champaign). It was prepared for use as described previously (Diaz et al., 2005).

Fluorescence Spectroscopy and Anisotropy Measurements

Corrected fluorescence spectra were acquired with a photon-counting Fluorolog-3-221 instrument (Jobin Yvon-Spex), using 1 nm excitation and 5 nm emission bandwidths, at 25°C. Fluorometric concentration measurements were made with a Shimadzu RF-540 spectrofluorometer. Anisotropy values were collected in the Fluorolog T-format mode with vertically polarized excitation and corrected for the sensitivity of each channel with horizontally polarized excitation (Lakowicz, 1999).

Binding of Taxoids to Microtubules

Binding constants of Hexaflutax to microtubules were obtained using anisotropy and centrifugation titration measurements. For the anisotropy measurements, 100 nM of Hexaflutax in 3.4 M glycerol, 10 mM sodium phosphate, 1 mM EGTA, and 0.1 mM GTP (pH 6.5) (GAB) was incubated for 30 min with increasing concentrations of binding sites in stabilized crosslinked microtubules (from 0 to 20 μM) at the desired temperature and the anisotropy of the solution was measured in a POLARSTAR BMG plate reader in the polarization mode, using the 480-P excitation filter and the 520-P emission filters. The bound fraction of Hexaflutax was calculated after correction for the different quantum yield of the bound and the free compound (Lakowicz, 1999). For the centrifugation measurements, 1 μM of binding sites in GAB were incubated for 30 min with increased concentrations of Hexaflutax (from 0 to 10 μM) in the presence and absence of 50 μM docetaxel. The samples were centrifugated for 20 min at 50,000 rpm in a TLA100 rotor in a Beckman Optima TLX centrifuge. The supernatants were taken and the pellets were resuspended in 50 mM phosphate buffer (pH 7.0) containing 1% SDS. The pellets and supernatants were diluted 1:5 in the same buffer and their fluorescence was measured using a Shimadzu RF-540 spectrofluorimeter (excitation wavelength 484 nm, emission wavelength 520 nm, 5 nm excitation and emission slits). The concentration of Hexaflutax in the samples was calculated using Hexaflutax spectrophotometric concentration standards. The bound concentration of Hexaflutax was considered to be that of the Hexaflutax in the pellets after correcting for the amount displaced by 50 μM docetaxel.

Binding constants of N-AB-PT to crosslinked stabilized microtubules were both measured using the Flutax-2 displacement method as described in Buey et al. (2005) and also by the change in their fluorescence intensity upon binding to microtubules (λexc 312 and λems 450 nm), in that case 200 nM of the compound was incubated with growing concentrations of crosslinked microtubules. The fractional saturation of the compound was estimated from the increase in their fluorescence intensity measured in a Fluorolog-3-221 instrument (Jobin Yvon-Spex).

Kinetics of Binding of Taxanes to Microtubules

The kinetics of binding and dissociation of taxanes to stabilized microtubules was measured by the change of intensity of fluorescence or the change in anisotropy of the fluorescence using a Bio-Logic SF300S stopped flow device equipped with a fluorescence detection system with an excitation wavelength of 495 nm and a filter with a cut-off of 520 nm in the emission pathway for Hexaflutax and the 4-4-20-Hexaflutax complex and with an excitation wavelength of 312 nm and a filter with a cut-off of 380 nm in the emission pathway for N-AB-PT paclitaxel, with polarizers in the optical pathways when the anisotropy change was measured. Appropriate photo bleaching controls were done. The fitting of the kinetic curves was done with a non-linear least-squares fitting program based on the Marquardt algorithm (Bevington, 1969).

Cell Biology Studies

Human A549 non-small lung carcinoma cells and human ovarian carcinomas A2780 and A2780AD (MDR overexpressing P-glycoprotein) were cultured as previously described (Buey et al., 2007).

Indirect immunofluorescence and cell cycle analysis was performed as described before (Buey et al., 2005). Cytotoxicity assays were performed with the MTT assay modified as described in Yang et al. (2007).

Homology Modeling

Sequences of human βI and βIII isotypes of tubulin were retrieved from the UniProt online database (UniProt-Consortium, 2009). Three dimensional models were thus generated from the 1JFF structure through homology modeling approaches by means of the Modeller9v5 python library (Sali and Blundell, 1993; Martí-Renom et al., 2000; Fiser et al., 2000; Eswar et al., 2006) according to the method already described to model the 3D structure of tubulin (*sus scrofa* sequence) (Magnani et al., 2009). A *very_fast* algorithm was used due to the high similarity showed by the selected human sequences (86%).

Each model was then refined by means of the "Protein Preparation Wizard" protocol of the Maestro suite (Mohamadi et al., 1990), selecting the most probable state at pH 7.0 ± 2 for protein residues. The position of each atom of the protein was relaxed through an energy minimization step carried out on the basis of the OPLS2005 force field (Jorgensen and Tirado-Rives, 1988; Kaminski et al., 2001), allowing for atom movements up to root mean square deviation displacement below 0.3 Å.

Docking Studies

All docking studies were performed with the AutoDock4 programs (v4.2.1) (Morris et al., 1998). Interaction grids were calculated for all the atom types of selected ligands with AutoGrid4 (v4.2.1) and were centered within the center of the so-called type I pore constituted by subunit α4, α3, β1, and β2 (Figure S3). Potential grid maps were of 25 × 25 × 35 Å dimensions, with a point spacing of 0.375 Å. Possible conformations of global energy minimum for tested molecules were generated toward the receptor surface, using a Lamarckian genetic algorithm (LGA), whereas free energies of binding were further calculated using the local search algorithm.

All LGA parameters were kept at the default values with the only exception being the maximum number of energy evaluations that was increased to 5 M, whereas the initial population for each generation step was enhanced to 250 individuals and the number of docking runs was set to 250.

For local search methods we performed 100 runs for each calculation, starting with an initial population constituted by 150 individuals. Coordinates of the ligand mass center, torsional dihedrals, and initial orientation were retained as those obtained by the docking results of the LGA methods.

Docking poses were clustered using a root mean square deviation tolerance of 2.0 Å.

Energy Minimization

All docking results were minimized with the MacroModel (Mohamadi et al., 1990) application of the Maestro Suite, using the AMBER* force field (Ferguson and Kollman, 1991; McDonald and Still, 1992) in implicit water solvent. The convergence criteria was set to the energy gradient of 0.01 kJ/Åmol or a maximum of 5000 iterations. An energy minimization step was further performed for each ligand and for all protein residues included within 3 Å from each ligand's atom, whereas an additional shell of residues (5 Å from the first shell) was restrained with a force constant of 200 $kJ \cdot Å^{-2} \cdot mol^{-1}$.

SUPPLEMENTAL INFORMATION

Supplemental Information includes five figures and one table can be found with this article online at doi:10.1016/j.chembiol.2010.02.006.

ACKNOWLEDGMENTS

We wish to thank S. Wang, M. Seisdedos, and P. Lastres for their technical assistance; F. Amat-Guerri for 7-Hexaflutax; E.W. Voss Jr. for the 4-4-20 anti-fluorescein monoclonal mouse IgG; and Rhône Poulenc Rorer Aventis for Docetaxel. We also would like to thank Matadero Municipal Vicente de Lucas de Segovia for providing the calf brains for tubulin purification. This work was supported in part by grant BIO2007-61336 from the Ministry of Science and Innovation to J.F.D., BIPPED-CM from Comunidad de Madrid to J.F.D. and J.M.A., and grant MOST No. 2006DFA31490 to W.S.F.

Received: November 30, 2009
Revised: January 26, 2010
Accepted: February 11, 2010
Published: March 25, 2010

REFERENCES

Andreu, J.M. (2007). Tubulin purification. In Methods in Molecular Medicine, J. Zhou, ed. (Totowa, NJ: Humana Press Inc.), pp. 17–28.

Bevington, P.R. (1969). Data reduction and error analysis for the physical sciences (New York: McGraw-Hill Book Co.).

Buey, R.M., Barasoain, I., Jackson, E., Meyer, A., Giannakakou, P., Paterson, I., Mooberry, S., Andreu, J.M., and Diaz, J.F. (2005). Microtubule interactions with chemically diverse stabilizing agents: thermodynamics of binding to the paclitaxel site predicts cytotoxicity. Chem. Biol. *12*, 1269–1279.

Buey, R.M., Calvo, E., Barasoain, I., Pineda, O., Edler, M.C., Matesanz, R., Cerezo, G., Vanderwal, C.D., Day, B.W., Sorensen, E.J., et al. (2007). Cyclostreptin binds covalently to microtubule pores and lumenal taxoid binding sites. Nat. Chem. Biol. *3*, 117–125.

Canales, A., Matesanz, R., Gardner, N.M., Andreu, J.M., Paterson, I., Diaz, J.F., and Jimenez-Barbero, J. (2008). The bound conformation of microtubule-stabilizing agents: NMR insights into the bioactive 3D structure of discodermolide and dictyostatin. Chemistry *14*, 7557–7569.

Diaz, J.F., and Andreu, J.M. (1993). Assembly of purified GDP-tubulin into microtubules induced by taxol and taxotere: reversibility, ligand stoichiometry, and competition. Biochemistry *32*, 2747–2755.

Diaz, J.F., Sillen, A., and Engelborghs, Y. (1997). Equilibrium and kinetic study of the conformational transition toward the active state of p21Ha-ras, induced by the binding of BeF3- to the GDP-bound state, in the absence of GTPase-activating proteins. J. Biol. Chem. *272*, 23138–23143.

Diaz, J.F., Strobe, R., Engelborghs, Y., Souto, A.A., and Andreu, J.M. (2000). Molecular recognition of taxol by microtubules. Kinetics and thermodynamics of binding of fluorescent taxol derivatives to an exposed site. J. Biol. Chem. *275*, 26265–26276.

Diaz, J.F., Barasoain, I., and Andreu, J.M. (2003). Fast kinetics of Taxol binding to microtubules. Effects of solution variables and microtubule-associated proteins. J. Biol. Chem. *278*, 8407–8419.

Diaz, J.F., Barasoain, I., Souto, A.A., Amat-Guerri, F., and Andreu, J.M. (2005). Macromolecular accessibility of fluorescent taxoids bound at a paclitaxel binding site in the microtubule surface. J. Biol. Chem. *280*, 3928–3937.

Eswar, N., Webb, B., Marti-Renom, M.A., Madhusudhan, M.S., Eramian, D., Shen, M.-Y., Pieper, U., and Sali, A. (2006). Comparative protein structure modeling using Modeller. Curr. Protoc. Bioinformatics, *Chapter* 5, Unit 5.6.

Evangelio, J.A. (1999). Interaction of microtubules with fluorescent taxanes. PhD thesis, Universidad Complutense de Madrid, Madrid, Spain.

Evangelio, J.A., Abal, M., Barasoain, I., Souto, A.A., Lillo, M.P., Acuna, A.U., Amat-Guerri, F., and Andreu, J.M. (1998). Fluorescent taxoids as probes of the microtubule cytoskeleton. Cell Motil. Cytoskeleton *39*, 73–90.

Ferguson, D.M., and Kollman, P.A. (1991). Can the Lennard-Jones 6-12 function replace the 10-12 form in molecular mechanics calculations? J. Comput. Chem. *12*, 620–626.

Fiser, A., Do, R.K.G., and Sali, A. (2000). Modeling of loops in protein structures. Protein Sci. *9*, 1753–1773.

Freedman, H., Huzil, J.T., Luchko, T., Luduena, R.F., and Tuszynski, J.A. (2009). Identification and characterization of an intermediate taxol binding site within microtubule nanopores and a mechanism for tubulin isotype binding selectivity. J. Chem. Inf. Model. *49*, 424–436.

Gaitanos, T.N., Buey, R.M., Diaz, J.F., Northcote, P.T., Teesdale-Spittle, P., Andreu, J.M., and Miller, J.H. (2004). Peloruside A does not bind to the taxoid site on beta-tubulin and retains its activity in multidrug-resistant cell lines. Cancer Res. *64*, 5063–5067.

Gutfreund, H. (1995). Kinetics for the Life Sciences (Cambridge: Cambridge University Press).

Hetenyi, C., and van der Spoel, D. (2002). Efficient docking of peptides to proteins without prior knowledge of the binding site. Protein Sci. *11*, 1729–1737.

Jorgensen, W.L., and Tirado-Rives, J. (1988). The OPLS potential functions for proteins—energy minimizations for crystals of cyclic-peptides and crambin. J. Am. Chem. Soc. *110*, 1657–1666.

Kaminski, G.A., Friesner, R.A., Tirado-Rives, J., and Jorgensen, W.L. (2001). Evaluation and reparametrization of the OPLS-AA force field for proteins via comparison with accurate quantum chemical calculations on peptides. J. Phys. Chem. B *105*, 6474–6487.

Kranz, D.M., and Voss, E.W., Jr. (1981). Partial elucidation of an anti-hapten repertoire in BALB/c mice: comparative characterization of several monoclonal anti-fluorescyl antibodies. Mol. Immunol. *18*, 889–898.

Lakowicz, J. (1999). Principles of Fluorescence Spectroscopy (New York: Kluwer Academic/Plenum Publishers).

Li, Y., Edsall, R., Jr., Jagtap, P.G., Kingston, D.G., and Bane, S. (2000). Equilibrium studies of a fluorescent paclitaxel derivative binding to microtubules. Biochemistry *39*, 616–623.

Magnani, M., Maccari, G., Andreu, J.M., Diaz, J.F., and Botta, M. (2009). Possible binding site for paclitaxel at microtubule pores. FEBS J. *276*, 2701–2712.

Martí-Renom, M.A., Stuart, A.C., Fiser, A., Sánchez, R., Melo, F., and Sali, A. (2000). Comparative protein structure modeling of genes and genomes. Annu. Rev. Biophys. Biomol. Struct. *29*, 291–325.

Matesanz, R., Barasoain, I., Yang, C., Wang, L., Li, X., De Ines, C., Coderch, C., Gago, F., Jimenez-Barbero, J., Andreu, J.M., et al. (2008). Optimization of taxane binding to microtubules. Binding affinity decomposition and incremental construction of a high-affinity analogue of paclitaxel. Chem. Biol. *15*, 573–585.

McDonald, D.Q., and Still, W.C. (1992). Amber* torsional parameters for the peptide backbone. Tetrahedron Lett. *33*, 7743–7746.

Mohamadi, F., Richards, N.G.J., Guida, W.C., Liskamp, R., Lipton, M., Caufield, C., Chang, G., Hendrickson, T., and Still, W.C. (1990). MacroModel an integrated software system for modeling organic and bioorganic molecules using molecular mechanics. J. Comput. Chem. *11*, 440–467.

Morris, G.M., Goodsell, D.S., Halliday, R.S., Huey, R., Hart, W.E., Belew, R.K., and Olson, A.J. (1998). Automated docking using a Lamarckian genetic algorithm and an empirical binding free energy function. J. Comput. Chem. *19*, 1639–1662.

Nettles, J.H., Li, H., Cornett, B., Krahn, J.M., Snyder, J.P., and Downing, K.H. (2004). The binding mode of epothilone A on alpha,beta-tubulin by electron crystallography. Science *305*, 866–869.

Nogales, E., Wolf, S.G., and Downing, K.H. (1998). Structure of the alpha beta tubulin dimer by electron crystallography. Nature *391*, 199–203.

Pryor, D.E., O'Brate, A., Bilcer, G., Diaz, J.F., Wang, Y., Kabaki, M., Jung, M.K., Andreu, J.M., Ghosh, A.K., Giannakakou, P., et al. (2002). The microtubule stabilizing agent laulimalide does not bind in the taxoid site, kills cells resistant to paclitaxel and epothilones, and may not require its epoxide moiety for activity. Biochemistry *41*, 9109–9115.

Sali, A., and Blundell, T.L. (1993). Comparative protein modeling by satisfaction of spatial restraints. J. Mol. Biol. *234*, 779–815.

Snyder, J.P., Nettles, J.H., Cornett, B., Downing, K.H., and Nogales, E. (2001). The binding conformation of Taxol in beta-tubulin: a model based on electron crystallographic density. Proc. Natl. Acad. Sci. USA *98*, 5312–5316.

Strehlow, H., and Knoche, W. (1977). Fundamentals of Chemical Relaxation (Weinheim, Germany: Verlag Chemie), pp. 101–105.

UniProt-Consortium. (2009). Universal Protein Resource (UniProt) 2009. Nucleic Acids Res. *37*, D169–D174.

Yang, C.G., Barasoain, I., Li, X., Matesanz, R., Liu, R., Sharom, F.J., Diaz, J.F., and Fang, W.S. (2007). Overcoming tumor drug resistance with high-affinity taxanes: a SAR study of C2-modified 7-acyl-10-deacetyl cephalomannines. ChemMedChem *2*, 691–701.